Chinese Chemical Letters 34 (2023) 108204

Contents lists available at ScienceDirect

Chinese Chemical Letters

journal homepage: www.elsevier.com/locate/cclet

Hybrid peroxi-coagulation/ozonation process for highly efficient removal of organic contaminants

Shasha Li[a,b,c], Jinxin Xie[a,b,c], Jinyu Gu[a,b,c], Minghua Zhou[a,b,c,*]

[a] Key Laboratory of Pollution Process and Environmental Criteria, Ministry of Education, College of Environmental Science and Engineering, Nankai University, Tianjin 300350, China
[b] Tianjin Key Laboratory of Environmental Technology for Complex Trans-Media Pollution, College of Environmental Science and Engineering, Nankai University, Tianjin 300350, China
[c] Tianjin Advanced Water Treatment Technology International Joint Research Center, College of Environmental Science and Engineering, Nankai University, Tianjin 300350, China

ARTICLE INFO

Article history:
Received 12 October 2022
Revised 18 January 2023
Accepted 8 February 2023
Available online 12 February 2023

Keywords:
Coal chemical industry wastewater
Phenol removal
Catalytic ozonation
Peroxi-coagulation
Reactive oxygen species

ABSTRACT

Aromatic compounds such as phenols presented widely in coal chemical industry wastewater (CCW) render the treatment facing great challenge due to their biorefractory characteristics and potential risks to the environment and human health. Ozone-based advanced oxidation processes show promising for these pollutants removal, but the mineralization *via* ozonation alone is unsatisfactory and not cost-effective. Herein, a hybrid peroxi-coagulation/ozonation process (denoted as PCO) was developed using sacrificial iron plate as an anode and carbon black modified carbon felt as cathode in the presence of ozonation. An enhanced phenol removal of ~100% within 20 min and phenol mineralization of ~80% within 60 min were achieved with a low energy consumption of 0.35 kWh/g TOC. In this novel process, synergistic effect between ozonation and peroxi-coagulation was observed, and beside O_3 direct oxidation, peroxone played a dominant role for phenol removal. In the PCO process, the hydrolyzed Fe species enhanced the generation of reactive oxygen species (ROS), while ·OH was dominantly responsible for pollutant degradation. This process also illustrated high resistance to high ionic strength and better performance for TOC removal in real wastewater when compared with ozonation and peroxi-coagulation process. Therefore, this process is more cost-effective, being very promising for CCW treatment.

Coal chemical industry wastewater (CCW), generated mainly from coal coking and coal gasification, is a typical industrial wastewater with great treatment difficulty [1]. Particularly, China has produced CWW around 475 million tons per year [2], containing high amounts of toxic chemicals and biorefractory matters with chemical oxygen demand (COD) and phenol concentration even up to 50,000 and 10,000 mg/L, respectively [3]. It can impose negative influence to environment and human health if improperly treated. Currently, the integrated systems combining conventional physicochemical process with biological process are the most widely used treatments technologies, but the unsatisfactory performance accompanied with high treatment cost has long been criticized. Therefore, it is imperative to develop efficient and low-cost CCW treatment process.

Advanced oxidation processes (AOPs), such as Fenton-like oxidation [4], electrochemical oxidation [5,6], wet oxidation [7] and photocatalytic oxidation [8,9] have been successfully applied to the treatment of CCW. However, several drawbacks are still encountered in utilizing AOPs methods. Fenton-like oxidation usually requires a pH of about 3 and is limited by the reduction of Fe(III). For photocatalytic oxidation, the inevitable problems are high investment cost, catalyst deactivation and catalyst recovery. Ozonation is one of the main technologies for refractory wastewater deep treatment and drinking water disinfection due to the excellent oxidation capacity of ozone (O_3, $E_0 = 2.07$ eV) [10]. Ozonation is increasingly used in industrial wastewater due to the gradual cost reduction for ozone production, and has been proven to be efficient to improve biodegradability of coal gasification wastewater [11]. However, ozone is a selective oxidant that can quickly oxidize organic compounds with electron-rich moieties such as phenols, olefins, and deprotonated amines [12,13]. The less reactivity for the small molecular weight compounds with carboxylic groups (rate constant of 0.01–100 L mol^{-1} s^{-1}) leads to low mineralization efficiency of contaminants [14].

* Corresponding author at: Key Laboratory of Pollution Process and Environmental Criteria, Ministry of Education, College of Environmental Science and Engineering, Nankai University, Tianjin 300350, China.
E-mail address: zhoumh@nankai.edu.cn (M. Zhou).

https://doi.org/10.1016/j.cclet.2023.108204
1001-8417/

As such, extensive efforts have been devoted to developing various processes to overcome this problem [15–17]. It is reported that the application of electric field can promote the decomposition of ozone to produce non-selective hydroxyl radical (•OH, $E_0 = 2.8$ V) as shown in Eqs. 1 and 2, thereby, degrading pollutants deeply into carbon dioxide and water [18,19]. Unfortunately, for high-salinity wastewater, the strong interaction between the soluble salts and the oxidative species leads to sluggish pollutant decomposition. Nevertheless, the soluble salts in CCW can act as an electrolyte for enhanced electrochemical process. In 2013, Wang *et al.* proposed electro-peroxone (EP) with *in-situ* generation of H_2O_2, which was reacted with the sparged ozone molecule to produce •OH (Eqs. 3 and 4) to degrade pollutants [20]. Since then, EP has been widely applied to dye removal [21], landfill leachate treatment [22], pharmaceuticals elimination [23,24], disinfection by-products control [25,26] and adsorbents regeneration [27,28]. Many works highlighted the process efficiency enhancement by peroxone resulting from H_2O_2 and O_3 reaction, but the formation efficiency of this reaction to •OH was only about 50% [29,30]. And some used anode materials such as boron-doped diamond (BDD) [31], dimensionally stable anode (DSA) [24] and Pt plate [22] are usually expensive, which limited its practical application.

$$O_3 + e^- \rightarrow {}^{\bullet}O_3^- \quad (1)$$

$${}^{\bullet}O_3^- + H_2O \rightarrow {}^{\bullet}OH + O_2 + OH^- \quad (2)$$

$$O_2 + 2H + e^- \rightarrow H_2O_2 \quad (3)$$

$$2O_3 + H_2O_2 \rightarrow 2{}^{\bullet}OH + 3O_2 \quad (4)$$

Sacrificial anode based on iron (Fe) or aluminum (Al) is a promising candidate to these expensive anodes for its low cost. Although electrocoagulation alone is hard to destroy dissolved organics, Fe(II) generated *in-situ* can catalytically active converting of O_3 or H_2O_2 (Eqs. 5–7) [32,33]. Xiong *et al.* [34] developed an electrolysis-assisted ozonation process by combining ozonation with electrocoagulation, showing excellent synergy on the abatement of *N*,*N*-dimethylacetamide (DMAC). In this process, H_2O_2 was supposed to be generated by the reduction of O_3 (Eqs. 8 and 9), and then reacted with O_3 or generated Fe^{2+} to form •OH, realizing the simultaneous ozonation, Fenton, peroxone oxidation and coagulation. Some studies further indicated that mutual promotion and synergy between ozone and coagulants (SOC) during the electro-hybrid ozonation-coagulation process with Al plate as anode and stainless steel as cathode [35], demonstrating that the ozonation and SOC effect were the main roles leading to the removal of ibuprofen at the initial pH of 5.

$$Fe^{2+} + O_3 \rightarrow FeO^{2+} + O_2 \quad (5)$$

$$FeO^{2+} + H_2O \rightarrow Fe^{3+} + {}^{\bullet}OH + OH^- \quad (6)$$

$$Fe^{2+} + H_2O_2 \rightarrow Fe^{3+} + {}^{\bullet}OH + OH^- \quad (7)$$

$$O_3 + OH^- \rightarrow O_2{}^{\bullet -} + HO_2{}^{\bullet} \quad (8)$$

$$2HO^{\bullet} \rightarrow O_2 + H_2O_2 \quad (9)$$

Additionally, the application of carbonaceous cathode is found to be capable of promoting the coupling effect of ozonation and electrochemical reduction by generating more H_2O_2 [36,37]. For example, Kong and co-workers [36] reported that the peroxi-coagulation coupled with ozonation process with Al plate as anode and C-PTFE as cathode could be used to treat shale gas fracturing flowback water, achieving a COD removal efficiency of 82.4% within 80 min at the current density of 50 mA/cm^2. These previous observations suggest that the combination of carbon-based cathode for H_2O_2 production and sacrificial anode might enhance the utilization of O_3 to improve the process efficiency due to the H_2O_2 exist widely, when compared with traditional electrocoagulation assisted ozonation process. Despite that, the peroxi-coagulation coupled with ozonation system has been rarely reported for CCW treatment as far as we known, not to mention the mechanism deep into the role of coagulation, catalytic oxidation and electrochemical reaction.

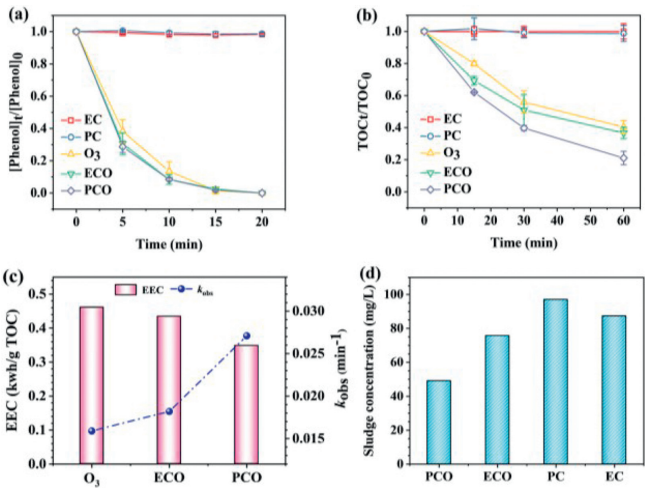

Fig. 1. (a) Phenol abatement. (b) TOC removal. (c) EEC and mineralization rate constants. (d) Sludge concentration for phenol degradation during O_3, EC, PC, ECO and PCO processes. Reaction conditions: $I = 10$ mA, initial pH 5.6 (uncontrolled), gas flow rate = 0.25 L/min, $t = 60$ min.

Herein, a hybrid peroxi-coagulation/ozonation process (PCO) was therefore proposed at a low current load using sacrificial iron plate as anode and carbon black modified carbon felt as cathode, which was efficient for *in-situ* H_2O_2 generation [38,39]. The main objective of this study was to evaluate the feasibility of PCO for CCW treatment and to elucidate the process mechanism, using phenol as the target pollutant since it was a typical pollutant in CCW. The performance by optimization of operation parameters, including ozone dosage, initial pH and co-existing anions were examined. The contributions of various reactions involved in the PCO were deduced based on the pseudo-first-order rate constant analysis. The feasibility for treatment of the real CCW by this PCO was further explored. This work would provide insight into the key factors and mechanism of the efficient PCO process.

To evaluate the superiority of the PCO process, it was compared with single ozonation and conventional electrocatalytic ozonation based on sacrificial anode for phenol removal. Fig. 1 shows the removal efficiency of phenol by ozonation (O_3), electrocoagulation (EC), peroxi-coagulation (PC), electrocoagulation coupled with ozonation (ECO) and PCO process. Apparently, the PCO had the biggest oxidation capacity among all processes. The removal and mineralization rate of phenol were negligible by EC and PC process after 60 min. For EC process, a possible explanation for this result was the almost non-availability of adsorption sites for the flocculants at high concentration of phenol [40]. Simultaneously, the •OH yield in EC and PC process was probably insufficient to destroy the molecular structure of pollutants. Although phenol could be completely removed within 20 min using ozonation alone, the TOC removal efficiency was unsatisfactory (60%). Combining EC with O_3, the mineralization efficiency of phenol by ECO increased to 63%. This result suggested that O_3 molecule could be catalyzed by the released iron ion, while the magnitude of this activation was insignificant. Interestingly, Fig. S2a (Supporting information) shows the accumulative concentration of H_2O_2 in DSA/Fe-O_2/O_3

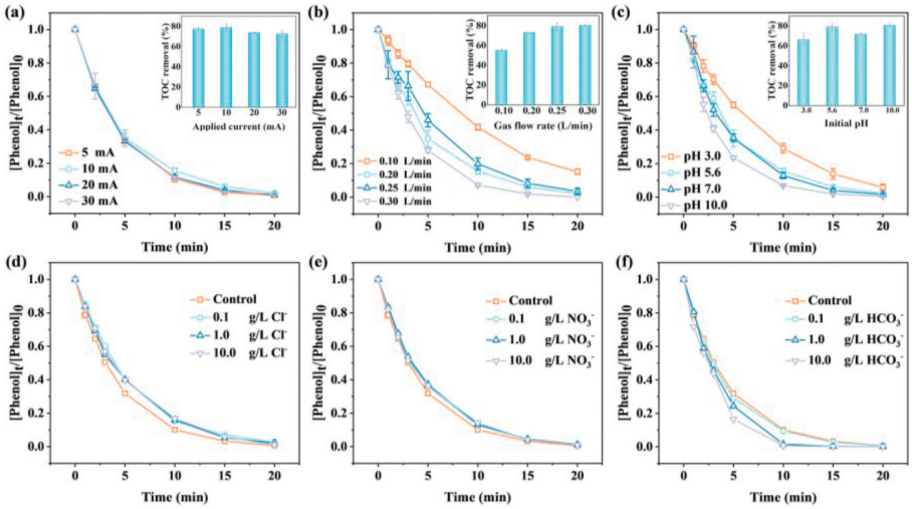

Fig. 2. Effects of the (a) applied current, (b) gas flow rate, (c) initial pH, (d) Cl^-, (e) NO_3^- and (f) HCO_3^- on the phenol removal during the PCO process. Reaction conditions: $I = 10$ mA, initial pH 5.6, gas flow rate = 0.25 L/min, $t = 60$ min.

was 1.29 mg/L at 30 min, while in DSA/Fe-O_2 system it almost approached zero. Thus it could be deduced that H_2O_2 was generated by the decomposition of O_3 rather than oxygen electrochemical reduction in the ECO system, which agreed well with the literature [34,41]. Remarkably, the residual concentration of H_2O_2 in ECO system was higher than the produced concentration in DSA/Fe-O_2/O_3 system, confirming the quick H_2O_2 decomposition in the presence of O_3 without pollutants. Further, the replacement of Fe plate cathode by modified carbon felt cathode could significantly accelerate the mineralization of phenol, achieving the mineralization efficiency of 79% at 60 min. This enhancement can be explained as the introduction of more H_2O_2 into the ECO process could catalyze the decomposition of O_3 (Fig. S3 in Supporting information). The lower residual H_2O_2 in the PCO process compared to ECO process also indicated that it had a higher H_2O_2 utilization efficiency (Fig. S2b in Supporting information).

Fig. 1c compared the phenol mineralization rate constant (k_{obs}-TOC) (see the detailed procedures in Fig. S4 in Supporting information) and electric energy consumption (EEC) during various processes. The EC and PC was not taken into consideration due to the poor phenol removal performance. The rate constant for phenol mineralization was about 0.0271 min^{-1} for PCO, which was 1.7 times and 1.5 times that of the ozonation (0.0159 min^{-1}) and ECO (0.0182 min^{-1}). Accordingly, the EEC for ozonation, ECO, and PCO were 0.46, 0.43, and 0.35 kWh/g TOC, respectively. Furthermore, it is well known that iron sludge will be produced by the iron-based AOPs system [42]. As illustrated in Fig. 1d, the PCO process achieved the lowest iron sludge generation of 49 mg/L at 60 min among all processes. The above results showed the superiority of the PCO process for phenol removal, *i.e.*, higher mineralization, lower EEC and iron sludge generation. In addition, the effects of applied current, the flow rate of ozone, initial pH and coexisting anions on phenol removal by PCO system has also been fully investigated, and the results were presented in Figs. 2a–f.

The applied current in the PCO process is a key parameter since it directly controls the production of Fe^{2+} on anode and the generation of H_2O_2 on the cathode, thereby affecting the removal of pollutants. As shown in Fig. 2a, the current had a slight of influence on the removal of phenol, which all reached 100% within 20 min at all applied currents. The mineralization efficiency of phenol accelerated when the applied current enlarged from 5 mA to 10 mA, in which a high TOC removal efficiency around 79% could be obtained. However, when the applied current rose from 10 mA to 30 mA, a decrease in TOC removal efficiency was observed (from 79% to 72%). This result could be attributed to the competition between flocculation and oxidation. The concentration of dissolved iron ion and the H_2O_2 production with the increased current was depicted in Fig. S5a (Supporting information). As expected, the increasing applied current could facilitate the generation of iron ion and H_2O_2, which would react with O_3 to promote $^{\bullet}OH$ generation [43,44]. However, excess H_2O_2 would consume some reactive species ($H_2O_2 + {}^{\bullet}OH \rightarrow {}^{\bullet}O_2H + H_2O$) [22]. Overall, a better phenol mineralization was not certainly realized by increasing the applied current. Conversely, it might be counterproductive since a high current would give rise to large iron sludge production and high energy consumption. As shown in Fig. S5b (Supporting information), the minimum energy consumption of 0.35 kWh/g TOC for phenol removal was obtained at the applied current of 10 mA. Therefore, from the perspective of economy and environmental protection, 10 mA was chosen as the best applied current.

The effects of ozone dosage in the sparged gas were investigated at the gas flow rate of 0.10–0.30 L/min. As shown in Fig. 2b, the removal of phenol varied greatly at different gas flow rate. Basically, increasing ozone dosage favored the phenol removal. The k_{obs} at the low gas flow rate of 0.10 L/min was only 0.093 min^{-1}, while it rapidly raised to 0.260 min^{-1} at the ozone flow rate of 0.30 L/min (Fig. S6 in Supporting information). Fig. 2b showed the TOC removal efficiency achieved 79% at ozone flow rate of 0.25 L/min. There are two possible reasons for the enhanced removal of phenol. One is the increase in mass transfer ratio of O_3 from gas phase to liquid phase as the ozone dosage increase, thereby, more O_3 exposure can be realized. Since ozonation can effectively oxidize phenol ($k = 100$ L mol^{-1} s^{-1}) [45], a significant improvement in phenol removal was observed as the O_3 exposure increased. Another is that more ROS were generated due to the enhanced O_3 mass transfer (including $^{\bullet}OH$ and $^{\bullet}O_2^-$) [46]. However, it should be noted that the improvement on phenol mineralization was not obvious when the gas flow rate increased from 0.25 L/min to 0.30 L/min, which might because the excessive O_3 could not be well utilized during the PCO process due to the limited solubility of O_3 in the solution [13]. Therefore, the optimal gas flow rate of 0.25 L/min was selected for the following experiments.

The initial pH plays a vital role in both ozonation and PC processes. Considering the much fluctuation of the pH value for real CCW generated from various coal chemical production technology [47], the removal of phenol by PCO was systematically investigated

at wide pH ranges of 3.0–10.0. As seen from Fig. 2c, the phenol removal all reached about 95%–100% within 20 min. Beyond that, 66%, 79%, 72%, and 81% of TOC were removed after 60 min at initial pH of 3.0, 5.6, 7.0 and 10.0, respectively. Apparently, there seemed to exist the initial pH value-dependent effect for TOC mineralization, *i.e.*, the higher the pH, the better the mineralization of phenol. By ozonation alone, the removal of organic pollutants under acidic conditions is dominated by direct ozonation [48]. The TOC removal efficiency by O_3 alone at initial pH of 3.0 was only 58% (Fig. S7a in Supporting information), a little lower than that by the PCO process (66%). These results showed that $^{\bullet}OH$ generation was prompted possibly because of the presence of Fe^{2+} or H_2O_2 in the PCO process. And the more $^{\bullet}OH$ production from O_3 decomposition under neutral and alkaline conditions contributed to the excellent performance of phenol mineralization [49]. The initial pH was one of the important factors affecting the existing forms of iron species. The variations of Fe^{2+}/Fe^{3+} ion during phenol removal upon different initial pH were depicted in Fig. S7b (Supporting information). The concentration of Fe^{2+} increased in the initial stage and then declined at all pH conditions, which could be ascribed to the transformation of iron species by precipitation and oxidation. As expected, as the reaction proceeded the Fe^{3+} concentration increased gradually (Fig. S7c in Supporting information). It reached 44 mg/L within 60 min at pH 5.6. Meanwhile, when increasing the initial pH, the concentration of both Fe^{2+} or Fe^{3+} at the same reaction time showed the similar decreasing trend. This phenomenon was reasonable since Fe was increasingly soluble at lower pH and the rate of $^{\bullet}OH$ generation during catalytic ozonation was also significantly corresponded to ferrous ion, which finally gave the intermediate Fe^{3+} [50]. The variation of Fe^{3+} can be explain by the fact that the precipitation of iron species more readily takes place at high pH conditions [51]. Given that the acceptable phenol removal without adjusting pH, there was no pH adjustment in later experiments except for the experiments on the effect of coexisting anions.

For real wastewater, the ubiquitous inorganic ions are a major challenge for the abatement of contaminants. Thus, three common anions chloride ion (Cl^-), nitrate ion (NO_3^-) and bicarbonate ion (HCO_3^-) with concentration range of 0.10–10.0 g/L (refer to the quality parameters of real CCW in Table S1 in Supporting information) were representatively added into the PCO system. As seen in Figs. 2d–f, the negligible effect of NO_3^- was observed even at an initial anion concentration of 10.0 g/L. Generally, the co-existing of Cl^- might promote the abatement of contaminants due to electrochemical production of reactive chlorine species (RCS), such as $^{\bullet}Cl$ and $^{\bullet}ClO$ [52]. When metals are used as anodes in electrolytic cells, the electron loss capability at anode follow the order of active metal > Cl^-, indicating that iron leaching before Cl^- being oxidized into RCS. Also, the coexisting Cl^- may slightly consume $^{\bullet}OH$ (Eq. 10), resulting in an inhibition effect on phenol removal. Thus, there was no enhancement on the phenol degradation in the presence of Cl^-. As a common quencher, despite HCO_3^- will consume $^{\bullet}OH$ in the solution, the phenol removal showed increasing trend with the increasing coexisting HCO_3^- concentrations, presumably due to the generation in a large number of $CO_3^{\bullet-}$ (Eq. 11), which could react with phenol with the second order rate constant values of $1.6 \times 10^7\ L\,mol^{-1}\,s^{-1}$ [53]. The above results showed that the PCO process exhibited high resistance to relatively high ionic strengths in real wastewaters.

$$Cl^- + {}^{\bullet}OH \rightarrow ClOH^{\bullet-} \quad (10)$$

$$^{\bullet}OH + HCO_3^- \rightarrow CO_3^{\bullet-} + H_2O \quad (11)$$

In the iron-based system, some high valent iron species, including Fe(V) and Fe(IV) might be generated, because Fe(IV) is supposed to be the primary oxidant for contaminant degradation [54]. First, PMSO, a high valent iron probe, was used as an indicator to detect the generated $^{\bullet}OH$ and high valent iron species in the process. As verified from the generated methyl phenyl sulfone ($PMSO_2$) concentration by different processes (Fig. S8 in Supporting information), the high valent-involved pathway should not occur in the process. After excluding the contribution of high valent iron to the phenol degradation, a series of EPR tests were performed to determine the ROS generated in the PCO process. As shown in Fig. 3a and Fig. S9a (Supporting information), the EPR spectrum of PCO exhibited obvious signal of DMPO-$^{\bullet}OH$ (1:2:2:1) and TEMP-$^1O_2$ adducts (1:1:1), which were generally assigned to the generation of $^{\bullet}OH$ and $^1O_2$, respectively [55]. As the electrolysis time increased, the signal intensity of DMPO-$^{\bullet}OH$ and TEMP-$^1O_2$ increased, indicating that $^{\bullet}OH$ and $^1O_2$ were continuously produced during the PCO process. Fig. S9b (Supporting information) showed that no obvious characteristic peaks of superoxide radicals ($^{\bullet}O_2^-$) were observed, therefore the contribution of $^{\bullet}O_2^-$ to phenol abatement was negligible. Overall, it was confirmed that $^{\bullet}OH$ and $^1O_2$ were possibly responsible for the phenol removal in the PCO process.

To further clarify the roles of ROS on the phenol removal and mineralization in the PCO process, a set of quenching experiments were performed by adding 4-chlorobenzoicacid (*p*-CBA), metronidazole (MDE) and hydrogen peroxide dismutase (CAT) as scavengers for $^{\bullet}OH$, $^1O_2$ and H_2O_2. Herein, *p*-CBA and MDE were used rather than *tert*-butanol and furfuryl alcohol to avoid the reaction mechanism change because of their low reactivity toward ozone ($< 0.1\ L\,mol^{-1}\,s^{-1}$, $< 1\ L\,mol^{-1}\,s^{-1}$), which had been widely used to calculate the exposures of ROS [56]. As illustrated in Fig. 3b, the presence of 0.5 mmol/L *p*-CBA decreased the phenol removal efficiency from 100% to 86% after 20 min reaction. The findings revealed that $^{\bullet}OH$ served as the main ROS for phenol degradation. When 0.5 mmol/L MDE was dosed into the system, the phenol removal was similar to that of MDE and *p*-CBA added together, implying that $^1O_2$ does little to the phenol degradation. It should be mentioned that CAT success to produce an inhibition on the phenol degradation to a certain extent, indicating that H_2O_2 as an auxiliary promoter was involved in the reaction. It is well known that H_2O_2 could be effectively produced at carbon-based cathode [57]. However, the presence of O_3 could influence the cathodic O_2 reduction [58]. From Fig. S10 (Supporting information), the cathodic O_3 reduction in modified carbon felt was more likely to be involved at considerably high potentials, which was in line with previous study [59]. Consequently, the cathodic potentials in desired low applied current were investigated. With the applied current increased from 0 mA to 10 mA, the cathodic potentials were decreased stepwise during electrolysis with either O_2 or O_2/O_3 sparging. The value was maintained at −0.45 V and −0.28 V (*vs.* Ag/AgCl), respectively. Notably, a relatively high cathode potential in the presence of O_2/O_3 was close to the onset cathodic oxygen reduction (−0.30 V *vs.* Ag/AgCl in Fig. S10a). This evidence confirmed that cathodic O_2 reduction could occur at low applied current of 10 mA during the PCO process. In particularly, the phosphate (PO_4^{3-}) was used to confirm the role of the surface hydroxyl groups of coagulants on the phenol removal. And the slight inhibition effect confirmed that the hydroxyl groups on coagulants could be the active sites for O_3 decomposition, which was further verified by the structures of the hydrolyzed Fe species in the subsequent section. Besides, $NaHSO_3$, an inorganic $^{\bullet}OH$ scavenger, was used to evaluate the role of $^{\bullet}OH$ for the phenol mineralization [60]. As presented in Fig. 3c, the removal efficiency within 60 min was 78% and 61% in the absence and presence of $NaHSO_3$, respectively, indicating that $^{\bullet}OH$ should work in the enhanced phenol mineralization in the PCO process. Also, DMSO was used as a free radical trapping agent to measure the $^{\bullet}OH$ generation with the electrolysis

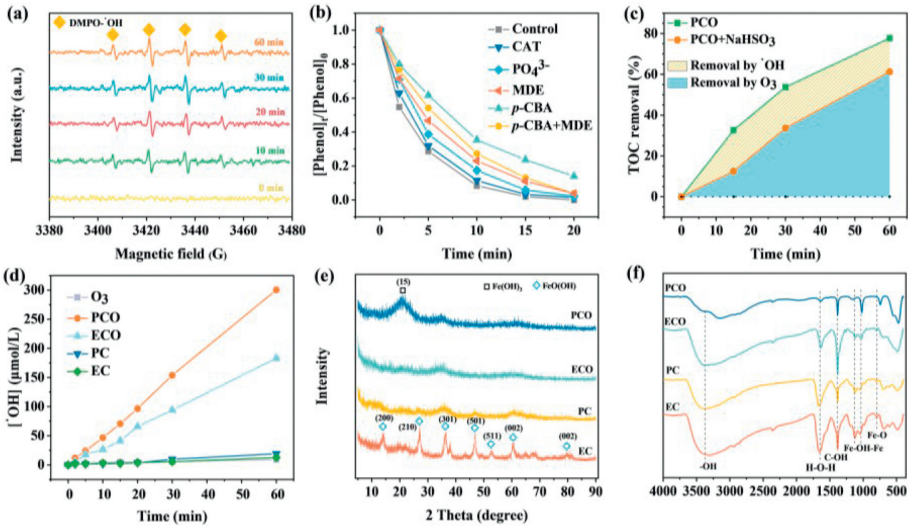

Fig. 3. (a) EPR spectra of PCO system in aqueous dispersion for DMPO-·OH adduct. (b) The quenching experiments with different scavengers. (c) The role of ·OH and O_3 for TOC removal during PCO process. (d) The cumulative concentration of ·OH with reaction time during different system; (e) XRD and (f) FTIR spectra of coagulants from different process. Reaction conditions: $I = 10$ mA, initial pH 5.6, [*p*-CBA] = [MDE] = 0.5 mmol/L, [CAT] = 500 U/mL, [PO_4^{3-}] = 1 g/L, gas flow rate = 0.25 L/min, $t = 60$ min.

time for different processes. As shown in Fig. 3d, the concentration of ·OH in the PCO process was always higher than other processes, revealing that the modified carbon felt cathode could enhance the hydroxyl radical generation due to more H_2O_2 generation, consistent with the mineralization results.

To further gain insight into the mechanism of the process, the XRD and FTIR spectra were employed to reveal the properties of the generated hydrolyzed Fe species from different processes without pH adjustment (Figs. 3e and f). It could be seen that there was different crystallinity for these coagulants. The diffraction peaks at 14.1° (200), 27.0° (210), 36.3° (301), 46.8° (501), 52.7° (511), 60.3° (002) and 79.6° (002) appeared on the EC by-product, which were attributed to the lepidocrocite (FeO(OH) [61]. While the diffraction peaks with a broad hump existed in the samples from the PC, ECO and PCO, indicating that these hydrolyzed products were amorphous or poorly crystalline in nature. In addition, the broad diffraction peaks at 21.2° were ascribed to the (200) plane of the magnetite (Fe_3O_4) in PCO by-product. In short, there were the mixture of magnetite and lepidocrocite in the coagulant from PCO process. As can be seen from Fig. 3f, the adsorption peaks at approximately 3400–3500 cm^{-1} and 1600–1640 cm^{-1} were observed for all the prepared coagulants, which could be related to the stretching vibration of chemically bonded -OH and the bending vibration of water molecules attached to the surface of the hydrolyzed Fe coagulants, respectively [62]. The adsorption band obtained in ranges of 1053–1211 cm^{-1} spectra corresponded to the Fe-OH-Fe bond. And the peaks around 692–706 cm^{-1} were attributed to the Fe-O [63]. Compared with ECO, the significant decreasing peak intensity in 1640 cm^{-1} showed that surface hydroxyl group served as the active sites for catalytic ozonation. This phenomenon can be explained as SOC effect. For example, several groups have reported that the Al-bonded or Fe-bonded surface hydroxyl groups (M-OH) is a type of strong Lewis acid sites that can react with ozone [64,65]. When high doses of ozone are added, an oxygen atom of the ozone molecule, acting as a Lewis base site, can be chemically adsorbed onto the M-OH, leading to the significantly declined peak intensities. The weaker peak intensity at about 1610 cm^{-1} in the PCO process than that of the PC further implied that O_3 consumed the -OH bond in coagulation from PCO. Accordingly, more surface hydroxyl groups were reacted in the PCO to be responsible for the generation of ROS (Eqs. 12–15), which was consistent with previous study [35]. At the same time, the C-OH group (1384 cm^{-1}) was all presented in five coagulants samples, proving the absorption of phenol or its intermediates on the surface of the coagulants.

$$\text{Fe-OH} + O_3 \rightarrow \text{Fe-OH-}O_3 \rightarrow \text{Fe-}O_2H^- + O_2 \quad (12)$$

$$\text{Fe-}O_2H^- + O_3 \rightarrow \text{Fe-}{}^{\bullet}O_2^- + HO_3{}^{\bullet} \quad (13)$$

$$\text{Fe-}{}^{\bullet}O_2^- + O_3 + OH^- \rightarrow \text{Fe-OH} + {}^{\bullet}O_3^- + O_2 \quad (14)$$

$${}^{\bullet}O_3^- + H^+ \rightarrow {}^{\bullet}HO_3^- \rightarrow {}^{\bullet}OH + O_2 \quad (15)$$

According to the above analyses, multiple reactions should occur for phenol removal in the PCO process, taking the following six reactions into consideration: EC, Fenton-like, O_3 direct oxidation (O_3), catalytic ozonation, peroxone reaction, and SOC. It is necessary to quantify the relative contributions of these reactions, adopting a method based on the proportion of the pseudo-first order rate constant (k_{obs}) of each reaction in the whole system [34]. In this case, the rate constant of phenol removal by different systems in the absence or presence of scavengers (*p*-CBA, CAT or phosphate) is listed in Table S2 (Supporting information), and the calculated contribution were summarized in Fig. S11 (Supporting information). Also, the analysis method was given in Table S3 (Supporting information).

In the EC process, coagulation was the only way for phenol removal. For the same applied current, Fe species was attained in almost the same amount by the EC and PCO process. Considering the poor phenol removal efficiency in EC process (Fig. 1), the contribution of coagulation in the PCO process should be negligible because the value of 0.007% was obtained by the proportion of k_{obs} of EC to the whole PCO process. In consideration of H_2O_2 formed in PC process, Fenton-like reactions could occur and the contribution of Fenton -like oxidation for phenol removal in PCO might be determined by the ratio of the difference between the k_{obs} of the PC and EC processes, which was only 0.3% in PCO process. However, there were no catalytic ozonation, peroxone, Fenton-like and SOC effect involved in the ·OH trapping experiments. Therefore, the proportion of O_3 direct oxidation could be calculated (37.6%). Furthermore, due to the coexistence of H_2O_2 and O_3, the peroxone reaction should be involved in the PCO process, and this reaction was gradually enhanced with the continuous production of H_2O_2 on the cathode. The removal of phenol with the addition of CAT was conducted to evaluate the contribution of peroxone. The k_{obs} of

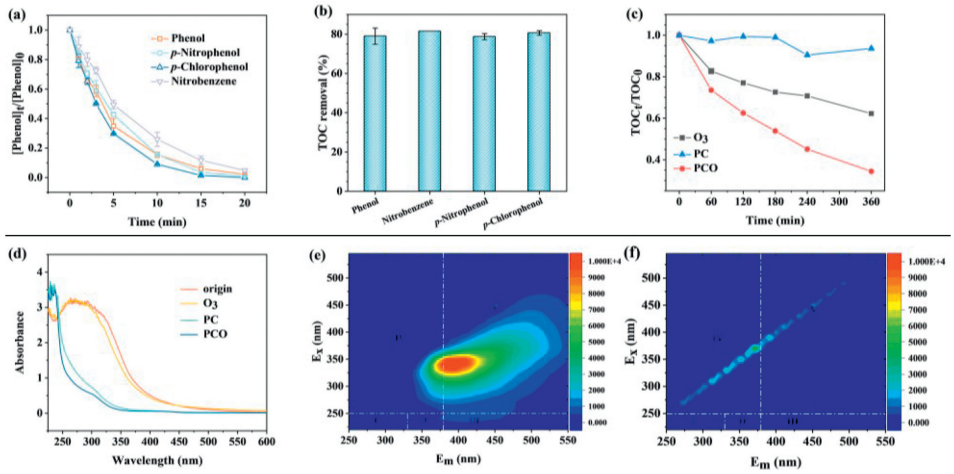

Fig. 4. (a) Pollutants abatement and (b) TOC removal for different pollutants. (c) TOC removal for real CCW. (d) UV absorption spectra of real CCW; EEM TOC spectrum of the (e) original CCW and (f) PCO system treated CCW after 60 min. Reaction conditions: $I = 10$ mA, initial pH 4.0 (uncontrolled), gas flow rate = 0.25 L/min, $t = 360$ min.

phenol removal obtained by PCO-CAT and PCO system were 0.258 and 0.218 min^{-1}, respectively, based on which the contribution of peroxone reaction could be acquired (15.1%). As an important part of the PCO process, the SOC effect was elucidated. The role of the hydroxyl groups on the surface of the hydrolyzed Fe species was eliminated by the addition of phosphate. Subsequently, the contribution from SOC effect was deduced based on the proportion of k_{obs} in PCO-phosphate and PCO system (26.7%). Moreover, the catalytic ozonation was responsible for the remaining phenol removal. Overall, the ozonation, SOC and catalytic ozonation played major roles in the PCO process under conditions without pH adjustment at applied current of 10 mA.

Besides phenol, aromatic compounds such as *p*-nitrophenol, nitrobenzene and *p*-chlorophenol are contained in CCW. They were thereby selected as the target pollutants to evaluate the feasibility of the PCO process in complex wastewater matrix. Fig. 4a showed that phenol, nitrobenzene, *p*-nitrophenol and *p*-chlorophenol were all well removed within 20 min. The corresponding pollutant mineralization efficiencies were 79%, 82%, 79% and 81%, respectively (Fig. 4b), which all much higher than that of ozonation alone (only 40%–60% TOC removal within 60 min) (Fig. S12 in Supporting information). These results supported that the PCO process possessed the enhanced performance for the removal of different pollutants.

To further confirm the applicability of the PCO process in real wastewater, the treatment of real CCW was conducted under the optimal conditions. As shown in Fig. 4c, the TOC mineralization efficiency of CCW reached 66% after 360 min treatment, and the TOC decreased from 157 mg/L to 54.0 mg/L. Compared to PC and ozonation, the TOC removal by PCO was significantly increased by 10 and 1.7 folds, respectively. The final organic content in treated CCW could meet the requirements on the evaporation and crystallization (COD < 200 mg/L) [66]. In addition, the treated CCW became clear and transparent. With regard to UV absorption spectra of raw CCW and effluents through different process shown in Fig. 4d, the raw CCW showed high absorption peaks within the range of 250 nm to 350 nm, which could be correlated to the presence of aromatic compounds such as phenols and polycyclic aromatic hydrocarbons [67]. The intensity of these peaks at the same wavelengths decreased evidently after treatment. A light color was observed, especially for the effluents by PCO, indicating the aromatic organics were removed. Further, the variations of fluorescence properties during the PCO treatment were evaluated. The original wastewater had three significant fluorescence peaks (III, IV and V) (Fig. 4e), indicating high content of fulvic acids-like, soluble microbial byproduct and humic acid-like substances in the raw CCW [68]. Apparently, the intensity at all regions in the excitation-emission matrix (EEM) fluorescence spectrum showed significant decrease after treatment of 360 min by PCO process (Fig. 4f), which might be caused by the relatively high reactivity of humic acid-like substances with ozone and $^{\bullet}OH$. The variations of fluorescence properties by PC and ozonation treatment can be found in the support information (Fig. S13). According to the similar EEM fluorescence spectra of PC-treated wastewater and raw CWW, the PC process had no significant removal of fluorescent substances. A slight intensity of fluorescence detection was still found for the Region III, IV and V during ozonation process. The above peak intensity changes in each process were in agreement with the TOC removal efficiency. All results suggested that the proposed PCO process was a promising alternative for treating CCW.

Table 1 presented the comparison of our work with the literature in the removal of contaminants using ozonation and electrocatalytic coupling process. The results show that the coupling process exhibits an excellent removal performance of phenol (100% within 20 min). The pseudo-first order rate constant (k_{obs}-TOC) for phenol mineralization of PCO system (0.027 min^{-1}) was found significantly better than traditional electrolysis coupled ozonation (0.014 min^{-1}). Moreover, conventional electrocatalytic ozonation processes generally have pretty pollutant removal performance in the range of applied current of 100–3000 mA, which could result in higher electrical energy consumption. This PCO process worked at a low current load (10 mA) and a 0.34 kwh/g TOC was required for phenol mineralization. Although the similar EEC to our works was obtained in electrocatalytic ozonation system using Pt plate, the electrode cost should be taken into account since Fe anode used in this study was cheaper. Hence, it would be a cost-effective system for the removal of contaminants using PCO process.

In the present work, a hybrid peroxi-coagulation/ozonation process was developed, demonstrating excellent performance for enhanced phenol removal and mineralization. The removal of phenol by PCO process was obtained 45-fold, 30-fold, 1.7-fold and 1.5-fold improvement on mineralization rate constant, inducing a significant enhancement compared to traditional EC, PC, ozonation and ECO process, respectively. The mainly responsible oxidants for phenol removal and mineralization were O_3, $^{\bullet}OH$. The multiple reactions of direct ozonation, SOC effect, catalytic ozonation, peroxone, coagulation and Fenton-like attributed to the removal, among which the former three were dominant. Meanwhile, the TOC removal efficiency obtained by the PCO process for real CCW validated the superiority than those of ozonation and PC process. In addition, the PCO process greatly reduced the amount of iron

Table 1
Comparison of the results with electrocatalytic ozonation system reported in the literatures.

Series	Anode material	Target pollutants	Reaction conditions		Removal performance			EEC (kWh/g TOC)	Refs.
			Ozone dosage	Current (mA)	Pollutants	TOC	k_{obs}-TOC (min^{-1})		
1	BDD	Phenol (0.9 L; 100 mg/L)	$[O_3]$ = 5 mg/L (0.05 L/min)	3000	–	~98% (1 h)	–	–	[10]
2	BDD	Phenol (1 L; 100 mg/L)	$[O_3]$ = 5 mg/L (0.05 L/min)	3000	~82% (1 h)	~100% (2 h)	–	0.45	[31]
3	Pt	Phenol (2 L; 100 mg/L)	$[O_3]$ = 53.55 mg/L (60 L/min)	100	~98% (1 h)	–	–	0.36	[41]
4	Ti-IrO_2	Phenol (1 L; 200 mg/L)	$[O_3]$ = 90 mg/L (0.4 L/min);	400	–	~64% (1 h)	0.014	–	[58]
5	Fe	(0.3 L; 200 mg/L)	$[O_3]$ = 55 mg/L (0.25 L/min)	10	~100% (20 min)	~80% (1 h)	0.027	0.35	This work

sludge at a low current load. This study demonstrated its wide application in efficient treatment of CCW.

Declaration of competing interest

We wish to confirm that there are no known conflicts of interest associated with this publication and there has been no significant financial support for this work that could have influenced its outcome.

Acknowledgments

This work was financially supported by Natural Science Foundation of China (Nos. 21976096 and 52170085), Key Project of Natural Science Foundation of Tianjin (No. 21JCZDJC00320), National high-level foreign experts project (Nos. QN20200002003, G2021125001 and G2021125002), and Fundamental Research Funds for the Central Universities, Nankai University.

Supplementary materials

Supplementary material associated with this article can be found, in the online version, at doi:10.1016/j.cclet.2023.108204.

References

[1] J. Shi, N. Wan, L. Li, Z. Li, H. Han, J. Clean Prod. 333 (2022) 130166.
[2] R. Xiong, C. Wei, J. Water, Process Eng. 19 (2017) 346–351.
[3] D. Li, J. Liu, J. Wang, et al., Cen. Asia-Pacific J. Chem. Eng. 13 (2018) e2162.
[4] H. Zhuang, H. Han, W. Ma, et al., J. Environ. Sci. 33 (2015) 12–20.
[5] Q. Zhao, F. Wei, L. Zhang, et al., Water Sci. Technol. 80 (2019) 836–845.
[6] K. Ning, J. Wang, X. Zeng, et al., J. Hazard. Mater. 430 (2022) 128379.
[7] V. Verma, P. Ghosh, S.B. Singh, V. Gupta, P.K. Chaudhari, Int. J. Chem. React. Eng. 20 (2022) 325–341.
[8] P. Xu, H. Xu, D. Zheng, Chem. Eng. J. 361 (2019) 968–974.
[9] W. Liu, Q. Liu, X. Li, Y. Song, W. Cao, Sci. China Technol. Sci. 53 (2010) 1477–1482.
[10] D. Amado-Piña, G. Roa-Morales, C. Barrera-Díaz, et al., Fuel 198 (2017) 82–90.
[11] Z. Yang, Y. Zhang, W. Zhu, et al., Chemosphere 255 (2020) 126963.
[12] Y. Zhang, E. Zhao, X. Cui, et al., Sep. Purif. Technol. 265 (2021) 118496.
[13] J. Song, N. Ma, W. Chen, J. Chen, Q. Dai, Sep. Purif. Technol. 282 (2022) 119969.
[14] Y. Wang, G. Yu, S. Deng, J. Huang, B. Wang, Chemosphere 208 (2018) 640–654.
[15] B. Wang, W. Shi, H. Zhang, H. Ren, M. Xiong, J. Environ. Chem. Eng. 9 (2021) 106115.
[16] N. Ma, Y. Ru, M. Weng, et al., Chemosphere 308 (2022) 136192.
[17] J. Wang, H. Liu, D. Ma, et al., Chemosphere 268 (2021) 128796.
[18] N. Kishimoto, Y. Morita, H. Tsuno, T. Oomura, H. Mizutani, Water Res. 39 (2005) 4661–4672.
[19] X. Li, Y. Li, H. Zhang, Chin. Chem. Lett. 32 (2021) 3221–3225.
[20] S. Yuan, Z. Li, Y. Wang, Electrochem. Commun. 29 (2013) 48–51.
[21] B. Bakheet, S. Yuan, Z. Li, et al., Water Res. 47 (2013) 6234–6243.
[22] Z. Li, S. Yuan, C. Qiu, et al., Electrochim. Acta 102 (2013) 174–182.
[23] Q. Yang, H. Huang, K. Li, et al., Chem. Eng. J. 415 (2021) 127618.
[24] Y. Zhang, S. Zuo, Y. Zhang, et al., J. Hazard. Mater. 368 (2019) 771–777.
[25] Y. Li, W. Shen, S. Fu, et al., Chem. Eng. J. 264 (2015) 322–328.
[26] Y. Zhang, S. Zuo, Y. Zhang, et al., Chem. Eng. J. 348 (2018) 485–493.
[27] M. Mustafa, I. Kozyatnyk, C. Gallampois, et al., Sci. Total. Environ. 776 (2021) 145723.
[28] X. Zhang, Y. Zhou, C. Zhao, et al., Chem. Eng. J. 304 (2016) 129–133.
[29] A. Fischbacher, J. von Sonntag, C. von Sonntag, T.C. Schmidt, Environ. Sci. Technol. 47 (2013) 9959–9964.
[30] J. Li, Y. Li, Z. Xiong, G. Yao, B. Lai, Chin. Chem. Lett. 30 (2019) 2139–2146.
[31] L. Hurtado, D. Amado-Piña, G. Roa-Morales, et al., J. Chem. 2016 (2016) 4108587.
[32] S. Zhou, L. Bu, Z. Shi, C. Bi, Q. Yi, Chem. Eng. J. 306 (2016) 719–725.
[33] M.R.K. Kashani, R. Kiani, A. Hassani, et al., Sep. Purif. Technol. 292 (2022) 121026.
[34] Z. Xiong, B. Lai, P. Yang, Water Res. 140 (2018) 12–23.
[35] X. Jin, X. Xie, Y. Liu, et al., Water Res. 177 (2020) 115800.
[36] F. Kong, X. Lin, G. Sun, et al., Chemosphere 218 (2019) 252–258.
[37] Y. Wang, F. Kong, D. Yang, et al., Chemosphere 262 (2021) 127968.
[38] F. Yu, M. Zhou, X. Yu, Electrochem. Acta 163 (2015) 182–189.
[39] X. Wang, J. Jing, M. Zhou, R. Dewil, Chin. Chem. Lett. 34 (2023) 107621.
[40] S. Vasudevan, J. Water. Process. Eng. 2 (2014) 53–57.
[41] O. Turkay, S. Barışçı, B. Öztürk, H. Öztürk, A. Dimoglo, J. Electrochem. Soc. 164 (2017) E180–E186.
[42] H. Monteil, Y. Péchaud, N. Oturan, M.A. Oturan, Chem. Eng. J. 376 (2019) 119577.
[43] C. Qu, G.S. Soomro, N. Ren, et al., J. Hazard. Mater. 384 (2020) 121398.
[44] C.V. Rekhate, J.K. Srivastava, Chem. Eng. Process. 165 (2021) 108442.
[45] J. Hoigné, H. Bader, Water Res. 17 (1983) 185–194.
[46] Q. Xiang, W. Cheng, S. Wen, et al., Water Res. 216 (2022) 118302.
[47] D. Maiti, I. Ansari, M. Rather, Deepa A, Water Sci. Technol. 79 (2019) 2023–2035.
[48] S. Yang, Y. Song, F. Chang, K. Wang, Environ. Res. 188 (2020) 109660.
[49] P. Fu, J. Feng, T. Yang, H. Yang, Miner. Eng. 81 (2015) 128–134.
[50] S. Song, Z. He, J. Qiu, L. Xu, J. Chen, Sep. Purif. Technol. 55 (2007) 238–245.
[51] Q. Zhang, M. Zhou, X. Du, et al., Chem. Eng. J. 429 (2022) 132436.
[52] H. Yin, Q. Zhang, Y. Su, Y. Tang, M. Zhou, Chem. Eng. J. 425 (2021) 131857.
[53] C. Busset, P. Mazellier, M. Sarakha, J. De Laat, J Photochem. Photobiol. A 185 (2007) 127–132.
[54] Z. Wang, W. Qiu, S. Pang, et al., Environ. Sci. Technol. 56 (2022) 1492–1509.
[55] P. Su, W. Fu, Z. Hu, J. Jing, M. Zhou, Appl. Catal. B Environ. 313 (2022) 121457.
[56] Y. Guo, J. Long, J. Huang, G. Yu, Y. Wang, Water Res. 215 (2022) 118275.
[57] W. Yang, M. Zhou, J. Cai, et al., J. Mater. Chem. A. 5 (2017) 8070–8080.
[58] G. Xia, H. Wang, J. Zhan, et al., Chem. Eng. J. 396 (2020) 125291.
[59] G. Xia, Y. Wang, B. Wang, et al., Water Res. 118 (2017) 26–38.
[60] H. Chen, Z. Zhang, D. Hu, et al., Chemosphere 265 (2021) 129047.
[61] J.A.G. Gomes, P. Daida, M. Kesmez, et al., J. Hazard. Mater. 139 (2007) 220–231.
[62] H. Eslami, M.H. Ehrampoush, A. Esmaeili, et al., J. Clean. Prod. 208 (2019) 384–392.
[63] T. Sun, C. Sun, G. Zhu, et al., Desalination 268 (2011) 270–275.
[64] X. Jin, Y. Liu, Y. Wang, et al., Chemosphere 253 (2020) 126625.
[65] M. Magureanu, D. Piroi, N.B. Mandache, et al., Appl. Catal. B: Environ. 104 (2011) 84–90.
[66] Z. Liu, L. You, X. Xiong, et al., Chemosphere 222 (2019) 696–704.
[67] X. Yu, R. Xu, C. Wei, H. Wu, J. Hazard. Mater. 302 (2016) 468–474.
[68] J. Zhou, J. Wang, A. Baudon, A.T. Chow, J. Environ. Qual. 42 (2013) 925–930.